Biology and Medicine
ISSN: 0974-8369

Tesfaye and Demlie, Biol Med (Aligarh) 2017, 9:2
DOI: 10.4172/0974-8369.1000380

Research Article Open Access

Insilco Modeling of Commonly Occurring Genetic Polymorphism of Human CYP3A4 on the Binding Affinity to UR-144

Amene Tesfaye[1*] **and Libargachew Demlie**[2]

[1]*Department of Pharmacy, Pharmacology Unit, College of Health Sciences, Jimma University, P. O. Box: 378, Jimma, Ethiopia*

[2]*Department of Chemistry, College of Natural and Computational Science, Mekelle University, P. O.Box:231, Mekele, Ethiopia*

[*]**Corresponding author:** Amene Tesfaye, Department of Pharmacy, Pharmacology Unit, College of Health Sciences, Jimma University, P. O. Box: 378, Jimma, Ethiopia, Tel: +251 47 111 1458; E-mail: amenet2009@gmail.com

Received date: December 01, 2016; **Accepted date:** February 06, 2016; **Published date:** February 13, 2017

Abstract

CYP3A4 accounts for about 30% in the human hepatic metabolism of xenobiotics. The defending mechanism of drug or xenobiotic metabolizing enzymes, particularly CYP superfamily has been found to be altered by both genetic polymorphisms and the environmental factors. The aim of this study was to examine UR-144 binding to CYP3A4 wild type and six different natural variants (I118V, R130Q, R162Q, D174H, T185S and L373F). A rigid ligand was docked by AutoDock Vina to flexible amino acid residues selected from the residues forming the binding pocket. The analysis of the docking results showed there is no difference in the binding affinities between the wild type and the natural variants. However, comparing the absolute binding affinity, the wild type (-12.8kcal/mol) has shown, among all, the lowest binding energy. Thus, this study depicts that the SNPs of CYP3A4 do not have any effects on the binding affinity of UR-144 to the active site.

Keywords: *Insilco*; Polymorphism; Autodock Vina; Synthetic cannabinoid

Introduction

CY3A4 is the most important drug or xenobiotic metabolising enzyme that plays a key role in the biotransformation of foreign compounds, which are introduced into the body for specific reasons [1]. CYP3A4 is one of the most abundantly expressed cytochromes in human liver contributing on average up to 30% to the microsomal pool of P450 system[2]. Therefore, owing to its broad substrate specificity, this enzyme is responsible for the metabolism of more than half the currently marketed drugs for human consumption. The purpose of CYP3A4 varies extensively both intra- and enter individually, thus contributing to unpredictable drug response and toxicity. CYP superfamily has been found to be altered by both genetic polymorphisms and the environmental factors [3].

UR-144 is a synthetic cannabinoid receptor agonist (SCRA) and has an affinity for CB1 and CB2 receptors. This particular drug has become popular due to its cannabimimetic effects through modulating the cannabinoid receptor. These effects are mediated through CB1 receptor coupled G-protein activation and finally result in decreased activity of cAMP dependent protein kinases [4]. UR-144 is a psychoactive with similar effect but, less potent than THC. This compound has been detected in herbal products marketed under a variety of names. It was only recently that this compound placed in Schedule I of the Controlled Substance Act. However, manufacturers kept to finding an alternative way of blending this molecule in an attempt to provide products that are still legal, resulting in a myriad of unusual chemicals that have never been evaluated scientifically. More importantly, there are no studies exist that demonstrate the safety of these drugs when consumed by humans [5-7].

The scientific knowledge that exists about UR-144 is very scarce. It is only recently, a study has shown that this compound is extensively metabolized by CYP3A4 at the tetramethylcyclopropyl (TMCP) moiety with minor contributions from CYP1A2. Besides, inhibition of CYP3A4 has showed the attenuation of UR-144 metabolism [8,9]. The main aim of the current work was to study *Insilco* binding affinity of UR-144 to CYP3A4 wild type and existing natural variants with single nucleotide polymorphism (SNP) using a computational approach.

Methods and Materials

Docking software

A Molecular Graphics Laboratory (MGL) tool [10] was used for the visualization and analysis of molecular structures. Auto Dock Vina [11] is a docking tool used to predict the interaction between small molecules, such as drug compounds or substrates, with the three-dimensional structure of a molecule.

Retrieval and preparation of CYP3A4 structure

The three-dimensional crystal structure of CYP3A4 was retrieved from RCBS PDB database (PDB ID: 1W0E, Resolution 2.80 Å) [12]. Prior to docking the structure of the wild and single nucleotide polymorphism were optimized by protein preparation wizard in Schrodinger Maestro Suite 2014 [13]. All water molecules were removed; polar hydrogen atoms and gassier charges were added to the protein for docking simulation. Optimization for incorrect bond, orientation of different functional groups of the amino acids was done.

Ligand molecule

In the present study, UR-144 was used as a ligand. The 3D structures of UR-144 were retrieved from the NCBI PubChem database with compound ID: 44626619 [14]. The ligand geometry and MM2 energy

minimization of the three-dimensional (3D) structure were performed to make it is suitable for docking using the ligand preparation application in Schrodinger Maestro Suite 2014 [13].

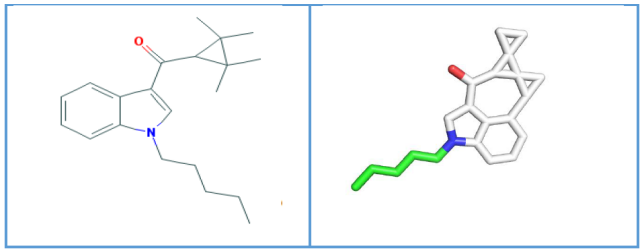

Figure 1: Chemical structure of UR-144 in two dimensions (Left) and three dimensions (Right).

Template identification and protein homology modeling

The FASTA sequence of five single nucleotide polymorphisms of CYP3A4 (I118V, R130Q, R162Q, D174H, T185S and L373F) were obtained from UniPortKB [15]. 3D structure of the wild CYP3A4 was built by Swiss model after target template alignment. We found that there is no 3D structure available for the selected SNP in Protein Data Bank; hence, we modeled the 3D structures of CYP3A4 with SNPs [16].The best template was selected based on sequence identity, domain coverage, and resolution, E-value. Based on sequence search and fold recognition, 1W0E, was selected as a template (>98% identity). Chimera interface to Modeler [17] was used for 3D structure generation based on the obtained information from sequence the alignment. HEM was added to all built structures, water and all other heteroatoms were removed. In this study, Modeler, generated 5 models and one model with lowest zDOPE value was selected to build the final 3D structure for docking.

Selection of flexible residues

In order to accommodate the entire flexible residue in and around active site, residues within 4.0 Å of resn HEM of the enzyme were selected manually. The resulting residues were screened to exclude those far from the active site. Finally, the following residues were set to be flexible for docking: L373, A370, D214, F215, T224, F108, I120, I301, F304, R212, G 480, G 481, L482, and L483. The flexible residues were generated by AutoDock tools and the resulting outputs file was saved as PDBQT files.

Docking protocol

UR-144 was docked into the active site of CYP3A4 after the water molecules were removed from the coordinates before docking. The binding site was defined after adding hydrogen molecules to generated CYP3A4 model receptors in order to describe the receptor cavity. The receptor file prepared with the addition of polar hydrogens, Kollman charges, and solvation parameters. The precalculated grid maps at the size set at 60, 60, and 60 Å (x, y, and z) to include all the amino acid residues that present in the receptor. The spacing between grid points was 0.375 angstroms. Docking was performed using AutoDock Vina and resulted models were visualized using PyMol [18].

Results and Discussion

The investigation of metabolic behavior and metabolism xenobiotic plays an important role in understanding the molecular mechanism of the chemical and its effect at large. Molecular docking, predicting the preferred orientation of one molecule into the second one, is frequently used to predict the binding orientation of small drug candidates to their protein targets [19]. Therefore, this method is suitable for the predicting the metabolic behavior through docking the compounds into the cavity of drug-metabolizing enzymes. The alignment of the amino acid sequence of the wild type and the selected SNPs are shown in Figure 2.

The LigPlot+ diagrams (Figure 3) shows the binding sites of proteins (1W0E) and the type of the bond that are formed in the binding pocket. This diagram can be interpreted as follows: the blue line - ligand bonds; red line - non ligand bonds; dotted lines -hydrogen bonds and its length; half red circle - non ligand residues involved in the hydrophobic contacts; black dots - corresponding atoms involved in the hydrophobic contacts. The LigPlot shows two of the SNPs (I 118 and R 130) that studied in this paper were part of the active residue in the binding pocket.

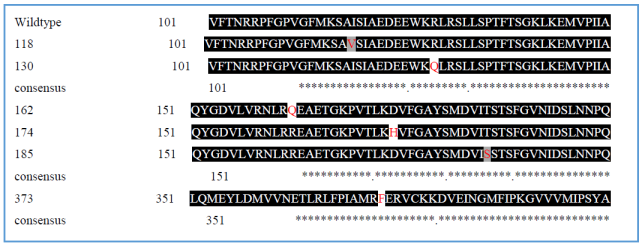

Figure 2: Multiple sequence alignment of CYP3A4 wild type, 118 I-V, 130 R-Q, 162 R-Q, 174 D-H and 373 L-F.

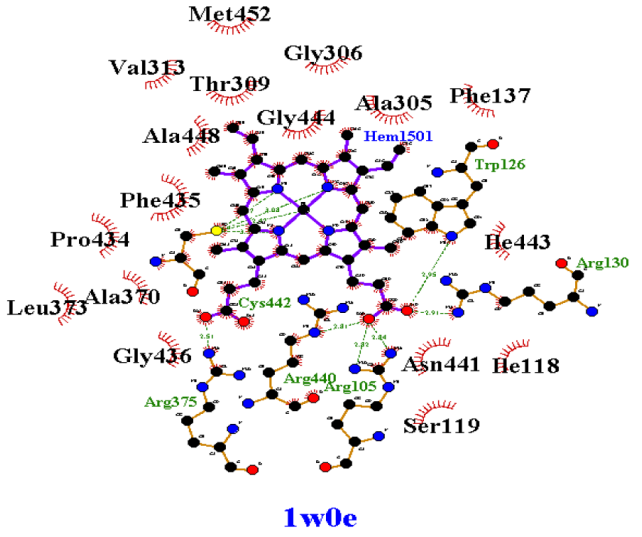

Figure 3: The LigPlot+ of 1W0E with HEM to predict important amino acid residue in and around the active binding site.

AutoDock Vina technique produced particular conformational sampling as a docking pose of the ligand molecule within the binding site, and an affinity (ΔG) describing the receptor ligand interaction strength. All docking poses were ranked according to their ΔG values, which ranged from -12.8 to -8.9 kcal/mol. The lowest binding energy from each pose is given in Table 1 for the entire model studied. The lowest binding energy was obtained for the wild type CYP3A4 followed by CYP3A4 SNP at L373 F.

In this study, two of the SNPs (I 118 and R130Q) were the residues at the active site of the enzyme. Though there is no specific study done on the synthetic cannabinoids and the aforementioned SNPs, different studies have shown that SNP at L373F displayed a significantly altered testosterone metabolite profile and a four-fold increase in the Km value for 1'-OH midazolam formation [20,21] lowest (-12.8 kcal/mol) and highest (-11.2 kcal/mol) binding energy were obtained for the wild type (Figure 4) and R162 Q (Figure 5) of CYP3A4 enzyme respectively.

Enzyme	Position	Description	Affinity (kcal/mol)
CYP3A4	Wild type	---------	-12.8
CYP3A4	118-118	I→ V	-11.4
CYP3A4	130-130	R → Q	-11.6
CYP3A4	162-162	R → Q	-11.2
CYP3A4	174-174	D → H	-12.3
CYP3A4	185-185	T → S	-11.9
CYP3A4	373-373	L → F	-12.7

Table1: Ligand binding free energy score of CYP3A4 wild type and SNPs docked with UR-144.

The results have shown that there is no difference in the binding affinity of the ligand to the wild form and other five natural variants of enzyme studied. The binding energy difference is within the standard error defined for AutoDock vina, which is ± 2.85 kcal/mol [18]. This agrees with report of different authors that the majority of SNPs have no biological consequences like substrate binding affinity to the active site of the enzyme [22,23].

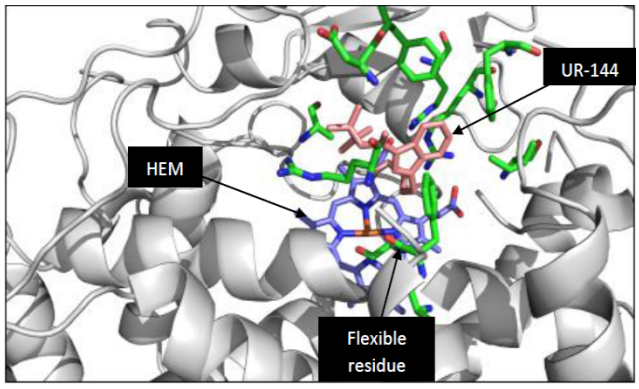

Figure 4: Structural view of docked complex of wild CYP3A4 and UR-144.

Clinical studies have shown the impact of the haplotype CYP3A4 harboring the T185S substitution on increase Paclitaxel metabolism [24]. Another studies, however, indicated that SNP at T185S have reduced *in vitro* catalytic activity for testosterone with lesser protein expression levels [25] and tanshinol borneol ester (DBZ) [26]. Moreover, previous studies had reflected that the SNP at this position may have involved in increasing or decreasing the catalytic activity of the enzyme. The current study has not shown a different binding affinity for these specific SNPs mentioned. The change R130Q was first identified in Caucasus with the frequency of 0.33% and the clinical impact of change have not yet indicated [27]. The present study has not shown binding affinity difference compared to the wild type.

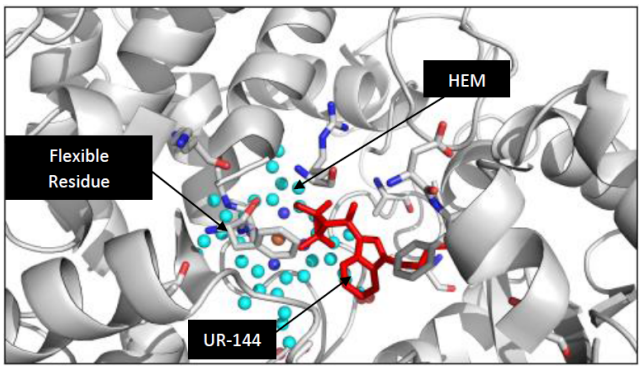

Figure 5: Structural view of docked complex 162 R- 162 Q SNP of CYP3A4 and UR-144.

Conclusion

The present study concludes that the studied SNPs of CYP3A4 do not have any effect on the binding affinity of UR-144 to the active site compared to the wild type. The lowest binding energy was obtained for the wild type followed by L373 F natural variant. However, further investigations and *in vivo* studies are needed to fully understand the metabolic pattern of UR-144.

Acknowledgments

The authors are thankful to European bioinformatics institute for providing LigPlot+ software for free and all the clarifications provided about the utilization.

References

1. Agúndez JAG, Klein K (2013) Functional polymorphisms of xenobiotics metabolizing enzymes-a research topic. Front Genet 4:79-81.
2. Subhani S and Jamil K (2015) Molecular docking of chemotherapeutic agents to CYP3A4 in non-small cell lung cancer. Biomed. Pharmacother 73: 65-74.
3. Klein K, Zanger UM (2013) Pharmacogenomics of cytochrome P450 3A4: Recent progress toward the "missing heritability" problem. Front Genet 4: 1-15.
4. World health organization (2014) UR-144.
5. Adamowicz P, Lechowicz W (2015) The Influence of Synthetic Cannabinoid UR-144 on Human Psychomotor Performance - A Case Report Demonstrating Road Traffic Risks. Traffic Inj Prev 16:754-759.
6. Vemuri VK, Makriyannis A (2015) Medicinal Chemistry of Cannabinoids. Clin Pharmacol Ther 97: 553-558.

7. Drug Enforcement Administration, Department of Justice (2016) Schedules of Controlled Substances: Placement of UR-144, XLR11, and AKB48 into Schedule I. Final rule. Fed Regist 81: 29142-29145.
8. Uchiyama N, Kawamura M, Kikura-Hanajiri R, Goda Y (2013) URB-754: A new class of designer drug and 12 synthetic cannabinoids detected in illegal products. Forensic Sci Int 227: 21-32.
9. Nielsen LM, Holm NB, Olsen L, Linnet K(2016) Cytochrome P450-mediated metabolism of the synthetic cannabinoids UR-144 and XLR-11. Drug Test Anal 8: 792-800.
10. Sanner MF (1999) Python: a programming language for software integration and development. J Mol Graphics Modell 17: 57-61.
11. Trott O, Olson AJ (2010) AutoDock Vina: improving the speed and accuracy of docking with a new scoring function, efficient optimization and multithreading. J Comput Chem 31: 455-461.
12. Yano JK, Wester MR, Schoch G A, Griffin KJ, Stout CD, et al. (2004) The structure of human microsomal cytochrome P450 3A4 determined by X-ray crystallography to 2.05-?? resolution. J Biol Chem 279: 38091-38094.
13. Sastry GM, Adzhigirey M, DayT, Annabhimoju R, Sherman W (2013) Protein and ligand preparation: Parameters, protocols, and influence on virtual screening enrichments. J Comput Aid Mol Des 27: 221-234.
14. https://pubchem.ncbi.nlm.nih.gov/compound/44626619#section=Top
15. UniProt Consortium (2015) UniProt: a hub for protein information. Nucleic Acids Res 43: D204-D212.
16. Kiefer F, Arnold K, Künzli M, Bordoli L, Schwede T (2009) The SWISS-MODEL Repository and associated resources. Nucleic Acids Res 37: D387-D392.
17. Pettersen EF, Goddard TD, Huang CC, Couch GS, Greenblatt DM, et al. (2004) UCSF Chimera - A visualization system for exploratory research and analysis. J Comput Chem 25: 1605-1612.
18. DeLano WL (2002) The PyMOL Molecular Graphics System;Version 1.1: Schrödinger LLC.
19. Eiselt R, Domanski TL, Zibat A, Mueller R, Presecan-Siedel E, et al. (2001) Identification and functional characterization of eight CYP3A4 protein variants. Pharmacogenomics J 11: 447-458.
20. Wang D, Sadee W (2012) The Making of a CYP3A Biomarker Panel for Guiding Drug Therapy. J Pers Med 2: 175-191.
21. Steffen C, Thomas K, Huniar U, Hellweg A, Rubner O, et al. (2010) TmoleX--a graphical user interface for TURBOMOLE. J Comput Chem 31: 2967-2970.
22. Fröhlich M, Hoffmann MM, Burhenne J, Mikus G, Weiss J, et al. (2004) Association of the CYP3A5 A6986G (CYP3A5*3) polymorphism with saquinavir pharmacokinetics. Br J Clin Pharmacol 58: 443-444.
23. Josephson F, Allqvist A, Janabi M, Sayi J, Aklillu E, et al. (2007) CYP3A5 genotype has an impact on the metabolism of the HIV protease inhibitor saquinavir. Clin Pharmacol Ther 81:708-712.
24. Nakajima Y, Yoshitani T, Fukushima-Uesaka H, SaitoY, Kaniwa N, et al. (2006) Impact of the haplotype CYP3A4*16B harboring the Thr185Ser substitution on paclitaxel metabolism in Japanese patients with cancer. Clin Pharmacol Ther 80: 179-191.
25. Lakhman SS, Ma Q, Morse G D (2009) Pharmacogenomics of CYP3A: considerations for HIV treatment. Pharmacogenomics J 10: 1323-1339.
26. Liu D, Gao Y, Wang H, Zi J, Huang H (2010) Evaluation of the effects of cytochrome P450 nonsynonymous single-nucleotide polymorphisms on tanshinol borneol ester metabolism and inhibition potential. Drug Metab Dispos 38: 2259-2265.
27. Jin T, Yang, H, Zhang J, Yunus Z, Sun Q, et al. (2015) Polymorphisms and phenotypic analysis of cytochrome P450 3A4 in the Uygur population in northwest China. Int J Clin Exp Pathol 8: 7083-7091.